

What is Generic Structure of the 3D Null-Point Magnetic Reconnection?

Yurii V. Dumin

*P.K. Sternberg Astronomical Institute (GAISH) of M.V. Lomonosov Moscow State University,
Universitetskii prosp. 13, 119992, Moscow, Russia*

and

*Space Research Institute (IKI) of Russian Academy of Sciences,
Profsoyuznaya str. 84/32, 117997, Moscow, Russia*

dumin@yahoo.com, dumin@sai.msu.ru

Boris V. Somov

*P.K. Sternberg Astronomical Institute (GAISH) of M.V. Lomonosov Moscow State University,
Universitetskii prosp. 13, 119992, Moscow, Russia*

somov@sai.msu.ru

ABSTRACT

The probability of occurrence of various topological configurations of the 3D null-point reconnection in a random magnetic field is studied. It is found that the non-axisymmetrical six-tail configuration (or “improper radial null”) should play the dominant role; while all other types of reconnection, in particular, the axially-symmetric fan-like structures (or “proper radial nulls”) are realized with a much less probability. A characteristic feature of the six-tail configuration is that at the sufficiently large scales it is approximately reduced to the well-known 2D X-type structure; and this explains why the 2D models of reconnection usually work quite well.

Subject headings: Magnetic fields — Magnetic reconnection — Sun: magnetic topology

1. INTRODUCTION

It is commonly recognized that reconnection of the magnetic field lines (Priest & Forbes 2000; Somov 2012, 2013, and references therein) is of fundamental importance in the dynamics of various astrophysical objects, ranging from planetary magnetospheres to interstellar medium, as well as in the laboratory plasmas (*e.g.*, Aulanier et al. 2000, 2007; Shibata et al. 2007; Eyink et al. 2013; Zhang et al. 2012; Walsh & Ireland 2003; Dumin 2002; Erdélyi & Ballai 2007; Olshevsky et al. 2013; Malakit et al. 2013; Egedal et al. 2012; Liu et al. 2013; Graham et al. 2014; Osman et al. 2014; Higashimori et al. 2013; Loureiro et al. 2013; Moser & Bellan 2012).

A classical mechanism of the magnetic recon-

nection assumes its development from the null (or “neutral”) point, where all components of the magnetic field \mathbf{B} disappear. (There are also some generalized models of reconnection which do not involve the null points at all, *e.g.*, as discussed by Priest et al. 2003; but we shall not consider such models in the present paper.)

Historically, the study of magnetic reconnection began from the 2D approximation, where the null points possessed a universal topology of X-type. However, starting from the mid 1990’s a considerable attention was paid also to the 3D case, where more diverse topological configurations are allowed (*e.g.*, review by Pontin 2011).

In the simplest case of a potential magnetic field, the structure of field lines in the vicinity of 3D null point can be pictorially presented as a col-

lision of two oppositely-directed magnetic fluxes with subsequent outflow in the equatorial plane. This outflow (or “fan”) can be either axially symmetric (which is called the “proper radial null” according to terminology by Parnell et al. 1996) or asymmetric (“improper radial null”).

It was implicitly assumed in many works that the most typical case of the 3D null point, which can serve as a good initial approximation, is just the axisymmetric fan-type structure (the proper radial null). On the other hand, a few recent papers (Al-Hachami & Pontin 2010; Pontin et al. 2011; Galsgaard & Pontin 2011) posed the problem of a “generic” 3D reconnection: they performed a numerical simulation of the magnetic fields whose initial configurations were substantially non-axisymmetric (*i.e.*, represented the improper radial nulls). Unfortunately, it remained unclear how important are such configurations from the statistical point of view? In other words, how often do they appear in a random magnetic field?

It is the aim of the present paper to provide a self-consistent calculation of the above-mentioned probabilities (and, thereby, to give a justification for reasonable choice of the initial field configurations in studies of the 3D magnetic reconnection).

2. THEORETICAL ANALYSIS

2.1. The Previous Treatments

A commonly-used approach to the analysis of the magnetic field structure in the vicinity of a null point is its expansion in Taylor series in the Cartesian coordinate system, whose origin is taken immediately in the null point:

$$B_i = \sum_j M_{ij} x_j, \text{ where } M_{ij} = \left. \frac{\partial B_i}{\partial x_j} \right|_{\mathbf{x}=0} \quad (1)$$

(*e.g.*, Gorbachev et al. 1988; Parnell et al. 1996, and references therein). Since the magnetic field \mathbf{B} must satisfy Maxwell equations, elements of the matrix \mathbf{M} are mutually related. In general, this matrix can be described by four independent parameters; see Eq. (14) in the above-cited paper by Parnell et al. (1996).

It can be intuitively assumed that the larger is the number of the parameters involved and the greater are the domains of their definition, the

larger will be the probability of realization of the respective field configuration. However, it is not so easy to justify this conjecture by using the representation (1): since elements of the matrix \mathbf{M} are mutually related by Maxwell equations, it is not clear how one should choose their joint probability distribution for the parameterization of the random field.

To get around this obstacle, it is necessary to use an explicit solution of the relevant field equations (*e.g.*, in terms of the spherical functions); so that the respective coefficients can be chosen as independent random variables. In the present paper, such an approach will be performed for the case of potential (current-free) magnetic field. A similar analysis for the non-potential field involves a more cumbersome mathematics and, therefore, requires a separate paper.

2.2. Initial Equations

We shall consider *random realizations* of the potential magnetic field

$$\mathbf{B} = -\text{grad } \psi, \quad (2)$$

where the magnetic potential ψ satisfies the usual Laplace equation:

$$\Delta\psi = 0. \quad (3)$$

(The potential field approximation is widely used, for example, in the solar physics, although it may be less relevant for treating the magnetospheric reconnection.)

Assuming the origin of spherical coordinate system (r, θ, φ) to be the spot of reconnection, solution of equation (3) can be written by the standard way as

$$\psi(r, \theta, \varphi) = \sum_{j=0}^{\infty} \sum_{m=0}^j r^j \psi_{jm}(\theta, \varphi), \quad (4)$$

where

$$\psi_{jm}(\theta, \varphi) = P_j^m(\cos \theta) [a_{jm} \cos(m\varphi) + b_{jm} \sin(m\varphi)] \quad (5)$$

are the spherical functions, and P_j^m are the adjoint Legendre polynomials. (The terms with negative powers of r are not taken into account because we are interested only in the nonsingular solutions.)

To avoid dealing with the infinite sum, it is convenient to assume that expression (4) is cut off at a sufficiently large value of j and, therefore, contains only the finite number of terms N . In other words, N is the dimensionality of the space of coefficients a_{jm} and b_{jm} .

If these coefficients are assumed to be random numbers, then we get a random realization of the magnetic field \mathbf{B} . It is a separate problem what are the reasonable probability distributions for these coefficients. However, it is important to emphasize that most of our subsequent results are based only on the dimensionality of various subsets of the coefficients a_{jm} and b_{jm} , which are responsible for the various kinds of reconnection. Therefore, the respective conclusions should be valid for any non-singular probability distributions.

Let us begin to analyze the terms of magnetic potential (4) with various powers of radius. At $j = 0$, we get $\psi^{(0)} = a_{00} = \text{const}$, which evidently does not affect any physical results.

Next, at $j = 1$, the magnetic potential is

$$\psi^{(1)} = r \{ a_{10} \cos \theta - (1 - \cos^2 \theta)^{1/2} [a_{11} \cos \varphi + b_{11} \sin \varphi] \}; \quad (6)$$

and its substitution into equation (2) results in

$$B_r^{(1)} = -\{ a_{10} \cos \theta - (1 - \cos^2 \theta)^{1/2} [a_{11} \cos \varphi + b_{11} \sin \varphi] \}. \quad (7)$$

Since $r = 0$ is assumed to be a null point (*i.e.*, all components of the magnetic field, including B_r , should vanish), we arrive at the requirement:

$$a_{10} = a_{11} = b_{11} = 0. \quad (8)$$

Because of these three constraints, *the null point of any kind will be realized only in a subspace of the random expansion coefficients a_{jm} and b_{jm} with dimensionality $N - 3$ or less.*

At $j = 2$, the magnetic potential is written as

$$\begin{aligned} \psi^{(2)} = r^2 \left\{ \frac{1}{2} (3 \cos^2 \theta - 1) a_{20} \right. \\ \left. - 3 \sin \theta \cos \theta [a_{21} \cos \varphi + b_{21} \sin \varphi] \right. \\ \left. + 3 \sin^2 \theta [a_{22} \cos(2\varphi) + b_{22} \sin(2\varphi)] \right\}. \quad (9) \end{aligned}$$

Since we are interested in structure of the magnetic field lines rather than in absolute values of

the field, it is convenient to introduce the normalized coefficients (denoted by a single subscript):

$$a_m = a_{2m}/a_{20}, \quad b_m = b_{2m}/a_{20}, \quad m = 1, 2. \quad (10)$$

Then, the magnetic field components take the form:

$$\begin{aligned} B_r^{(2)} = -2a_{20}r \left\{ \frac{1}{2} (3 \cos^2 \theta - 1) \right. \\ \left. - \frac{3}{2} \sin(2\theta) [a_1 \cos \varphi + b_1 \sin \varphi] + \right. \\ \left. + 3 \sin^2 \theta [a_2 \cos(2\varphi) + b_2 \sin(2\varphi)] \right\}, \quad (11a) \end{aligned}$$

$$\begin{aligned} B_\theta^{(2)} = -3a_{20}r \left\{ \sin(2\theta) \left[-\frac{1}{2} + a_2 \cos(2\varphi) \right. \right. \\ \left. \left. + b_2 \sin(2\varphi) \right] - \cos(2\theta) [a_1 \cos \varphi + b_1 \sin \varphi] \right\}, \quad (11b) \end{aligned}$$

$$\begin{aligned} B_\varphi^{(2)} = -3a_{20}r \left\{ 2 \sin \theta [-a_2 \sin(2\varphi) + b_2 \cos(2\varphi)] \right. \\ \left. + \cos \theta [a_1 \sin \varphi - b_1 \cos \varphi] \right\}. \quad (11c) \end{aligned}$$

2.3. Asymptotic Directions

Following the standard procedures, the equation of a magnetic field line can be written as

$$\frac{dr}{B_r/(a_{20}r)} = \frac{r d\theta}{B_\theta/(a_{20}r)} = \frac{r \sin \theta d\varphi}{B_\varphi/(a_{20}r)}. \quad (12)$$

Since quantities $B_r^{(2)}/(a_{20}r)$, $B_\theta^{(2)}/(a_{20}r)$, and $B_\varphi^{(2)}/(a_{20}r)$ do not depend on r , in the limit $r \rightarrow 0$ we arrive at the conditions specifying *the field lines passing immediately through the null point*:

$$B_\theta^{(2)}/(a_{20}r) = 0, \quad B_\varphi^{(2)}/(a_{20}r) = 0. \quad (13)$$

Substitution of the detailed expressions (11b) and (11c) into (13) gives the following set of algebraic equations:

$$\begin{aligned} \sin(2\theta^*) \left[-\frac{1}{2} + a_2 \cos(2\varphi^*) + b_2 \sin(2\varphi^*) \right] \\ - \cos(2\theta^*) [a_1 \cos \varphi^* + b_1 \sin \varphi^*] = 0, \quad (14a) \end{aligned}$$

$$\begin{aligned} 2 \sin \theta^* [-a_2 \sin(2\varphi^*) + b_2 \cos(2\varphi^*)] \\ + \cos \theta^* [a_1 \sin \varphi^* - b_1 \cos \varphi^*] = 0, \quad (14b) \end{aligned}$$

where θ^* and φ^* are the angles at which the field line enters (or leaves) the null point.

First of all, it can be easily checked that the above set of equations is preserved under the

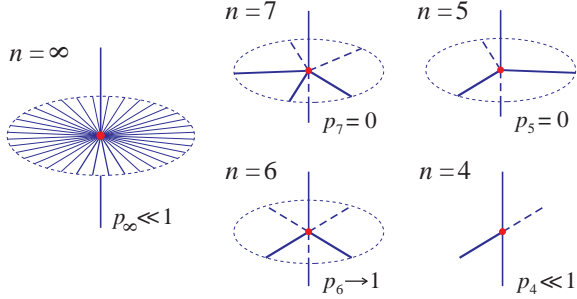


Fig. 1.— Sketch of the various hypothetical null points, comprising both the axially-symmetric fan-like configuration (left) and a few structures with the finite number of asymptotic directions n (right).

transformation: $\theta^* \rightarrow \pi - \theta^*$, $\varphi^* \rightarrow \varphi^* + \pi$. Consequently, the magnetic field lines passing through the null point always appear as the oppositely-directed pairs. So, the geometric structures with an odd number of tails (e.g., $n = 5$ or 7 in Figure 1) cannot exist at all.

Next, let us analyze the particular solutions of equations (14a) and (14b). The simplest case evidently takes place at $a_1 = b_1 = a_2 = b_2 = 0$ or, in the original designations,

$$a_{2m} = 0, b_{2m} = 0, \text{ where } m = 1, 2. \quad (15)$$

Then, these equations are reduced to the simple condition

$$\sin(2\theta^*) = 0, \quad (16)$$

which has solutions of the two types:

$$\theta^* = 0, \pi \quad \text{and} \quad \theta^* = \pi/2 \quad (\text{at any } \varphi^*). \quad (17)$$

This represents a combination of the polar axis and a disk in the equatorial plane, i.e., exactly the axially-symmetric fan-like structure depicted in the left-hand side of Figure 1. (It is called “the proper radial null” according to terminology by Parnell et al. 1996.)

Because of the 4 constraints (15), this structure seems to be realized in the subspace of coefficients a_{jm} and b_{jm} with dimensionality $N - 3 - 4 = N - 7$. However, it should be born in mind that these constraints were formulated for the specific situation when “spine” of the “fan” was oriented exactly along the polar axis of the coordinate system used. In general, such fan-like structure can

be rotated in space by two Euler angles, which effectively removes 2 constraints. So, the dimensionality of the relevant subset of coefficients will be $N - 7 + 2 = N - 5$.

Returning to the general case of arbitrary coefficients a_1, b_1, a_2 , and b_2 , it can be naturally assumed that the set of two algebraic equations (14a) and (14b) for two unknown variables θ^* and φ^* should have a finite number of solutions (i.e., the number of asymptotic tails in Figure 1 should be finite). Moreover, as follows from a more careful mathematical analysis, this number is always equal to 6 (except for some special subset of coefficients a_i and b_i with lower dimensionality).

To prove this fact, it is convenient to reduce the above-mentioned system of equations to a single equation for the azimuthal angle φ^* :

$$F(\eta(\varphi^*), \zeta(\varphi^*)) = 0, \quad (18)$$

where $\eta = \cos \varphi^*$, $\zeta = \sin \varphi^*$, and

$$\begin{aligned} F(\eta, \zeta) = & 4[2a_2\eta\zeta - b_2(\eta^2 - \zeta^2)](a_1\zeta - b_1\eta) \\ & \times \left[-\frac{1}{2} + a_2(\eta^2 - \zeta^2) + 2b_2\eta\zeta\right] \\ & - \left\{4[2a_2\eta\zeta - b_2(\eta^2 - \zeta^2)]^2 - (a_1\zeta - b_1\eta)^2\right\} \\ & \times (a_1\eta + b_1\zeta). \end{aligned} \quad (19)$$

Then, if the roots φ^* have been found, the corresponding values of the polar angle θ^* can be easily restored from one of equations (14a) or (14b).

Since formula (19) represents a quite complex polynomial expression, the simplest approach to resolve our task is just to perform a statistical simulation: let us generate a sufficiently large sequence of random coefficients a_1, a_2, b_1 , and b_2 (e.g., as a Gaussian distribution with a zero mean) and then analyze behavior of the function $F(\eta(\varphi^*), \zeta(\varphi^*))$ graphically (Figure 2). Surprisingly, it was found that the plot of F intersects the horizontal axis always in 3 points at the interval $\varphi^* \in [0, \pi]$ (and, consequently, in 6 points at the interval $\varphi^* \in [0, 2\pi]$). In fact, a subsequent careful analysis enabled us to get a rigorous mathematical proof of this fact. However, because of the cumbersome formulas, it will be not presented here, and we prefer to appeal just to the results of statistical simulation. Besides, it was established that the above-mentioned six solutions of the equations (14a) and (14b) correspond geomet-

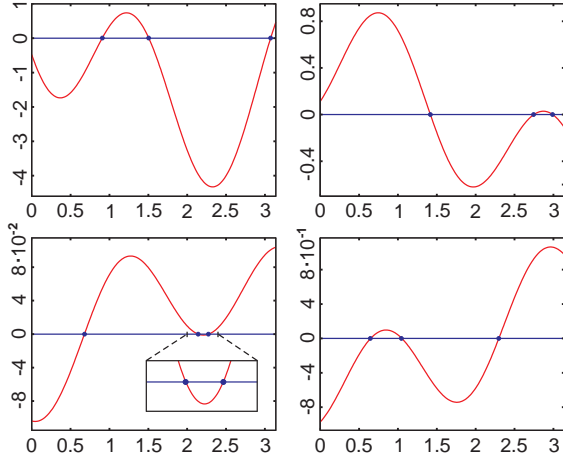


Fig. 2.— A few examples of the function $F(\eta(\varphi^*), \zeta(\varphi^*))$ at the interval $\varphi^* \in [0, \pi]$ at random values of the coefficients a_1, a_2, b_1 , and b_2 .

rically to the six “tails” which are mutually orthogonal to each other.

Therefore, we have found that a *generic 3D null point* in the potential field approximation should have a specific six-tail structure (*i.e.*, possess 6 asymptotic directions of the magnetic field). This is because it is realized in the subspace of coefficients of the random field with dimensionality $N - 3$, *i.e.*, almost in the entire space allowed for the null point by the constraints (8). All other configurations (in particular, the intuitively attractive axially-symmetric fan or more exotic geometric structures outlined in the old paper by Zhugzhda 1966) should emerge with a much less probability, because they are realized in the subsets of coefficients with lower dimensionality. It is especially important to emphasize that, since these conclusions are based only on the dimensionality of the relevant subspaces, they should be valid for any nonsingular probability distribution of the random-field coefficients. (So, the particular Gaussian distribution used in the simulation presented in Figure 2 does not affect the final result.)

2.4. Structure of the Field Lines

It is important, of course, to discuss a pattern of the magnetic field lines *in the vicinity* of the above-mentioned generic configuration. To avoid cumbersome formulas, let us consider the simplest

(but completely representative) case $a_1 = b_1 = b_2 = 0, a_2 \neq 0$, which corresponds to the six-tail structure oriented along the axes of the coordinate system. Then, equations (14a) and (14b) are simplified to

$$\sin(2\theta^*) \left[-\frac{1}{2} + a_2 \cos(2\varphi^*) \right] = 0, \quad (20a)$$

$$a_2 \sin \theta^* \sin(2\varphi^*) = 0. \quad (20b)$$

Their solutions are evidently $\theta^* = 0, \pi$ and $\theta^* = \pi/2$, $\varphi^* = 0, \pi/2, \pi, 3\pi/2$, which correspond just to the six semiaxes of the coordinate system.

Next, omitting the unessential common multiplier a_{20} , expressions (11a)–(11c) for the magnetic field components are reduced to

$$B_r = -2r \left[\frac{1}{2} (3 \cos^2 \theta - 1) + 3a_2 \sin^2 \theta \cos(2\varphi) \right], \quad (21a)$$

$$B_\theta = -3r \sin(2\theta) \left[-\frac{1}{2} + a_2 \cos(2\varphi) \right], \quad (21b)$$

$$B_\varphi = 6a_2 r \sin \theta \sin(2\varphi). \quad (21c)$$

As expected, B_θ and B_φ vanish immediately at the coordinate axes, while B_r changes its sign on the opposite sides from the origin.

Substituting expressions (21a)–(21c) into (12) and performing the integration, we can easily find formulas for the magnetic field lines in three coordinate planes. For example, in the xy -plane ($\theta = \pi/2$) the final result will take the form:

$$r = C \left(|\sin \varphi|^{1-1/(6a_2)} |\cos \varphi|^{1+1/(6a_2)} \right)^{-1/2}, \quad (22)$$

where C is an arbitrary constant. Behaviour of this function has three qualitatively different regimes, depending on the value of coefficient a_2 :

- (a) If $a_2 < -1/6$ or $a_2 > 1/6$, then $r \rightarrow \infty$ both at $\varphi \rightarrow 0$ and $\varphi \rightarrow \pi/2$. This evidently corresponds to the field line of hyperbolic type.
- (b) If $-1/6 < a_2 < 0$, then $r \rightarrow \infty$ at $\varphi \rightarrow 0$ and $r \rightarrow 0$ at $\varphi \rightarrow \pi/2$. This is the field line of parabolic type with the parabola axis oriented in x -direction.
- (c) If $0 < a_2 < 1/6$, then $r \rightarrow 0$ at $\varphi \rightarrow 0$ and $r \rightarrow \infty$ at $\varphi \rightarrow \pi/2$. This is also the field line of parabolic type but with the parabola axis oriented in y -direction.

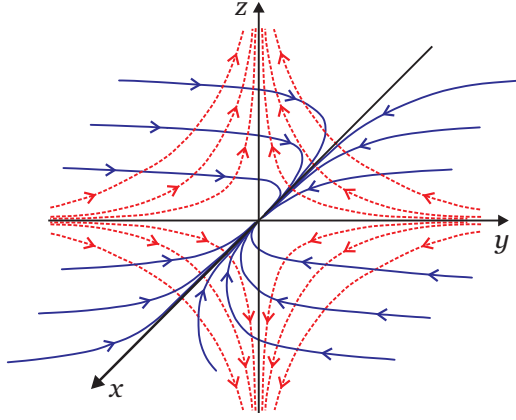


Fig. 3.— Sketch of magnetic field lines in the six-tail configuration. Solid (blue) curves represent the field lines in the horizontal xy -plane; and dotted (red) curves, in the vertical yz -plane. Field lines in another vertical plane xz , perpendicular to the plane of figure, are not shown here; they have the same hyperbolic structure as in the yz -plane.

As regards the field lines in two other coordinate planes, they can be shown to have a hyperbolic structure in cases (b) and (c). Just this situation is illustrated in Figure 3.

Furthermore, it can be proved that the same pattern of the field lines can be associated with all other cases mentioned above just by interchanging the role of various coordinate axes. Using the terminology adopted in the theory of differential equations, one can say that the field lines have a node structure in one of the coordinate planes and the saddle structure in two other planes.

Let us emphasize that the six-tail arrangement of the magnetic field lines in the vicinity of a 3D null point is not a new finding: this configuration is well known from the earlier works, *e.g.*, Figure 1 in paper by Gorbachev et al. (1988) or Figure 5 in paper by Parnell et al. (1996)), where it was called “the improper radial null”. However, it has not been recognized up to now that just this structure should play the dominant role in the 3D magnetic reconnection.

Besides, the previously-used term “improper” looks somewhat misleading in the case that is actually the most typical. So, we prefer to call it “the six-tail configuration”. In fact, the purely

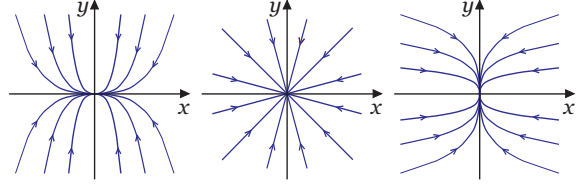


Fig. 4.— Appearance of the axially-symmetric fan as the intermediate case between two six-tail configurations. Only field lines in the xy -plane are drawn here; the field lines in the xz - and yz -planes always remain of the saddle type.

geometric aspects of this structure may be studied more efficiently by the employment of Taylor expansion in Cartesian coordinates (1); for more details, see Section III in the above-cited paper by Parnell et al. (1996). On the other hand, our approach, based on the spherical functions, makes it possible to perform an accurate statistical parameterization of the random magnetic field and, thereby, to calculate the respective probabilities.

2.5. Pictorial Illustration

It can be easily understood why probability of occurrence of the axially-symmetric fan-type structure (left-hand panel in Fig. 1) should be substantially suppressed as compared to the six-tail structure. Really, let us pay attention to the behavior of field lines in the xy -plane of Figure 3 and assume that initially the value of parameter a_2 corresponded to the case (c), as depicted in the left-hand panel of Figure 4. Next, let a_2 gradually decrease and become negative, which refers to the case (b). From the geometric point of view, this corresponds to a gradual decrease in curvature of the field lines, and at some instant they become bent in another direction, *i.e.*, the entire pattern remains parabolic but the parabola axis jumps by $\pi/2$ (right-hand panel in Figure 4). Then, the boundary between these two cases is just the axially-symmetric fan-type structure, depicted in the central panel, which is realized at $a_2 = 0$.

In other words, there are infinitely many six-tail configurations of types (b) and (c) but only one intermediate axially-symmetric fan-type configuration. So, the probability of its realization should be extremely small. (This picture is quite

similar to Figure 2 by Priest & Titov 1996, who used the magnetic field parameterization in Cartesian coordinates.)

2.6. Reduction to Quasi-2D Geometry

Returning to Figure 3, attention should be paid to the fact that six asymptotic directions of the magnetic field are quite different from each other. Namely, four of them (y , $-y$, z , and $-z$) can be called “dominant”, because most of the field lines tend to approach one of these directions when they go away from the null point. On the other hand, two other asymptotic directions (x and $-x$) should be called “recessive”, because most of the field lines tend to depart from them. Therefore, the recessive directions will be “lost” when observed from a large distance, and the entire pattern will look like a classical 2D X-point. This fact can explain why the 2D models of magnetic reconnection usually work rather well.

For example, Masson et al. (2009) performed a numerical simulation of the solar flare presumably caused by a single null point and have found that the respective 3D reconnection actually proceeds in the quasi-two-dimensional slabs. The same reduction to a quasi-2D configuration was observed very clearly in our numerical simulations of bifurcation of the 3D null points in the solar atmosphere (Dumin & Somov 2015, in preparation).

3. CONCLUSIONS

We have calculated the probability of occurrence of various kinds of the 3D null points in a random magnetic field and studied the structure of field lines in their vicinity. As a result, it was found that:

1. Contrary to the intuitive expectations, the most likely case of the 3D null point, responsible for the magnetic reconnection, is the specific six-tail structure (or “the improper radial null”, according to terminology by Parnell et al. 1996).
2. All other kinds of the 3D null points, in particular, the intuitively attractive axially-symmetric fan (or “proper radial null”) are realized with much less probabilities, as schematically summarized in Figure 1.

3. At the sufficiently large distances, the generic six-tail structure is approximately reduced to a quasi-2D configuration of the well-known X-type, which explains why the 2D approach is often a good approximation for the magnetic reconnection. Therefore, it may be conjectured that the specific 3D effects should be important, first of all, in the small-scale magnetic reconnection events (*e.g.*, in the solar micro- and nano-flares).

One of the authors (YVD) is grateful to J. Büchner, A.T. Lukashenko, D.D. Sokoloff, and I.S. Veselovsky for fruitful discussions and comments. We are also grateful to the unknown referee for valuable bibliographic suggestions.

REFERENCES

- Al-Hachami A. K., & Pontin D. I. 2010, *A&A*, 512, A84
- Aulanier, G., DeLuca, E. E., Antiochos, S. K., McMullen, R. A., & Golub, L. 2000, *ApJ*, 540, 1126
- Aulanier, G., Golub, L., DeLuca, E. E., et al. 2007, *Science*, 318, 1588
- Dumin, Yu.V. 2002, *Adv. Space Res.*, 30, 565
- Egedal, J., Daughton, W., & Le, A. 2012, *Nature Phys.*, 8, 321
- Erdélyi, R., & Ballai, I. 2007, *Astron. Nachr.*, 328, 726
- Eyink, G., Vishniac, E., Lalescu, C., et al. 2013, *Nature*, 497, 466
- Galsgaard K., & Pontin, D. I. 2011, *A&A*, 534, A2
- Gorbachev, V. S., Kel’ner, S. R., Somov, B. V., & Shvarts, A. S. 1988, *Soviet Ast.*, 32, 308
- Graham, D. B., Khotyaintsev, Yu. V., Vaivads, A., André, M., & Fazakerley, A. N. 2014, *Phys. Rev. Lett.*, 112, 215004
- Higashimori, K., Yokoi, N., & Hoshino, M. 2013, *Phys. Rev. Lett.*, 110, 255001
- Liu, Y.-H., Daughton, W., Karimabadi, H., Li, H., & Roytershteyn, V. 2013, *Phys. Rev. Lett.*, 110, 265004

- Loureiro, N. F., Schekochihin, A. A., & Zocco, A. 2013, *Phys. Rev. Lett.*, 111, 025002
- Malakit, K., Shay, M. A., Cassak, P. A., & Ruffolo, D. 2013, *Phys. Rev. Lett.*, 111, 135001
- Masson S., Pariat E., Aulanier G., & Schrijver C. J. 2009 *ApJ*, 700, 559
- Moser, A. L., & Bellan, P. M. 2012, *Nature*, 482, 379
- Olshevsky, V. S., Lapenta, G., & Markidis, S. 2013, *Phys. Rev. Lett.*, 111, 045002
- Osman, K. T., Matthaeus, W. H., Gosling, J. T., et al. 2014, *Phys. Rev. Lett.*, 112, 215002
- Parnell, C. E., Smith, J. M., Neukirch, T., & Priest, E. R. 1996, *Phys. Plasmas*, 3, 759
- Pontin, D. I. 2011, *Adv. Space Res.*, 47, 1508
- Pontin D. I., Al-Hachami, A. K., & Galsgaard K. 2011, *A&A*, 533, A78
- Priest, E., & Forbes, T. 2000, *Magnetic Reconnection: MHD Theory and Applications* (Cambridge, UK: Cambridge Univ. Press)
- Priest, E., Hornig, G., & Pontin, D. I. 2003, *J. Geophys. Res. A*, 108, 1285
- Priest, E. R., & Titov, V. S. 1996, *Phil. Trans. R. Soc. Lond. A*, 354, 2951
- Shibata, K., Nakamura, T., Matsumoto, T., et al. 2007, *Science*, 318, 1591
- Somov, B. V. 2012, *Plasma Astrophysics, Part I: Fundamentals and Practice* (2nd ed., NY: Springer)
- Somov, B. V. 2013, *Plasma Astrophysics, Part II: Reconnection and Flares* (2nd ed., NY: Springer)
- Walsh, R. W., & Ireland, J. 2003, *A&A Rev.*, 12, 1
- Zhang, T. L., Lu, Q. M., Baumjohann, W., et al. 2012, *Science*, 336, 567
- Zhugzhda, Yu. D. 1966, *Geomagnetism i Aeronomiya*, 6, 506 (in Russian)